

This article was downloaded by:

On: 30 January 2011

Access details: *Access Details: Free Access*

Publisher *Taylor & Francis*

Informa Ltd Registered in England and Wales Registered Number: 1072954 Registered office: Mortimer House, 37-41 Mortimer Street, London W1T 3JH, UK



## Separation & Purification Reviews

Publication details, including instructions for authors and subscription information:

<http://www.informaworld.com/smpp/title~content=t713597294>

## Electric Field Control of Membrane Transport and Separations

A. J. Grodzinsky<sup>a</sup>; A. M. Weiss<sup>a</sup>

<sup>a</sup> Continuum Electromechanics Group Department of Electrical Engineering and Computer Science, Massachusetts Institute of Technology, Cambridge, Massachusetts

**To cite this Article** Grodzinsky, A. J. and Weiss, A. M. (1985) 'Electric Field Control of Membrane Transport and Separations', *Separation & Purification Reviews*, 14: 1, 1 — 40

**To link to this Article: DOI:** 10.1080/03602548508068410

**URL:** <http://dx.doi.org/10.1080/03602548508068410>

## PLEASE SCROLL DOWN FOR ARTICLE

Full terms and conditions of use: <http://www.informaworld.com/terms-and-conditions-of-access.pdf>

This article may be used for research, teaching and private study purposes. Any substantial or systematic reproduction, re-distribution, re-selling, loan or sub-licensing, systematic supply or distribution in any form to anyone is expressly forbidden.

The publisher does not give any warranty express or implied or make any representation that the contents will be complete or accurate or up to date. The accuracy of any instructions, formulae and drug doses should be independently verified with primary sources. The publisher shall not be liable for any loss, actions, claims, proceedings, demand or costs or damages whatsoever or howsoever caused arising directly or indirectly in connection with or arising out of the use of this material.

## ELECTRIC FIELD CONTROL OF MEMBRANE TRANSPORT AND SEPARATIONS

A. J. Grodzinsky and A. M. Weiss  
Continuum Electromechanics Group  
Department of Electrical Engineering and Computer Science  
Massachusetts Institute of Technology  
Cambridge, Massachusetts 02139

### I. INTRODUCTION

This review focuses on a relatively new class of membrane separation processes in which an electric field applied across a charged membrane can control the permeability of that membrane to charged and neutral solutes in real time. Of particular interest is the identification of various mechanisms that enable such electric field control of membrane permeability. Devices based on this principle have potentially important applications in the area of actively controlled time variable membrane separation and drug delivery systems, as well as low energy analytical and preparative systems. In addition, applied fields can also affect the concentration polarization layer (gel layer) associated with ultrafiltration membranes.

In the area of membrane transport, electrical forces can couple to charged membrane macromolecules and interstitial fluid (e.g., electrokinetic interactions),<sup>1</sup> or directly to charged solute species (e.g., solute migration). It is therefore very important to distinguish between the effect of an electric field on the membrane matrix versus that on the solutes to be transported. To make this

point, we will highlight several contrasting systems including one in which the spacing between molecules of a membrane matrix, and hence the effective pore radius of the membrane, can be controlled by an applied field. More specifically, the electric field in this latter configuration alters the neutral salt concentration or pH inside the membrane by means of an electrodiffusion mechanism. This modulates electrostatic repulsion forces between charged membrane molecules and fibrils, thereby changing the interstitial separation distances which determine the effective permeability of the membrane to other neutral or charged solute probes. This is an example of a system in which the applied field directly affects the properties of the membrane; hence, even the transport of neutral solutes can be changed.

One embodiment of this system has been tested using a theoretical model for membrane transport along with independent measurements of field-related transport properties.<sup>2</sup> Experimental results show that changes in membrane swelling and hydration (which can be produced electrically or chemically) are accompanied by measurable changes in the flux of labeled solutes.<sup>2</sup> Thus, the electric field acts as a switch to control the swelling state and the permeability of the membrane.

In order to put into perspective the various roles that can be played by an applied electric field, we will first review certain changes in membrane properties that can be induced by chemical means alone. For example, salt concentration, pH, and the binding of specific reagents to membrane molecules (all of which can be modulated by applied electric fields) have important effects on membrane hydration, morphology, and permeability to fluids and solutes. Examples of such phenomena from the biological literature will also be described, as they provide interesting clues concerning the importance of hindered diffusion of large solutes in the problem of electric field control. Finally, membrane separation and reaction processes based on the use of transmembrane electric fields will be discussed, including electroactive polymer membranes and electrodiffusion-control of membrane transport. Recent

experimental advances in the use of real-time fluorescence methods to investigate membrane transport are presented.

## II. CHEMICAL CONTROL OF MEMBRANE PERMEABILITY

Several novel studies have shown that membrane transport properties can be controlled by adjusting the chemical constituents of the membrane bath.

### 1. Polyelectrolyte-bound Membranes

Pefferkorn et al.<sup>3</sup> observed that a pH controlled helix-coil conformational transition in poly( $\alpha$ ,L-glutamic acid) molecules that had been irreversibly adsorbed onto the pore walls of cellulose acetate (Millipore) filters could alter the filter's hydraulic permeability, membrane potential and  $^{22}\text{Na}^+$  sorption properties. The conformational change was brought about by ionization of the anionic polyelectrolyte molecule. For pH < 5, stiff helical chains were pictured to have most of their segments in direct contact with the pore surface. After ionization at higher pH, coiled molecular loops extended into the pore fluid thereby reducing hydraulic permeability by as much as a factor of two for membranes having a pore radius of 0.05 $\mu\text{m}$  and a thickness of 127 $\mu\text{m}$ .

### 2. Collagen Membranes

In the experiments of Pefferkorn et al.,<sup>3</sup> the membrane pores were rigid but could be blocked by conformational changes in adsorbed, flexible macromolecules. In contrast, others have studied membranes made entirely of flexible molecules in which ionization of fixed charge groups can result in bulk swelling of the membrane. Gliozzi, Ciferri and their coworkers<sup>4-6</sup> have used collagen protein membranes that were cast from a dispersion of steer tendon fibrils. These membranes could undergo a crystalline-to-amorphous (denaturation) phase transition depending on bath pH, salt type and concentration, and temperature. Bartolini et al.<sup>4</sup> observed changes

of several hundred per cent in the sucrose permeability and hydraulic filtration of 25 $\mu$ m thick doubly oriented collagen films in baths of concentrated  $\text{CaCl}_2$ , as the solution concentration was increased from 1 to 5 molar through the phase transition point. They also found that isothermal variations in length and swelling accompanied the melting transition observed as the  $\text{CaCl}_2$  concentration was increased. Hence, they concluded that their membrane's structure and physical properties were closely linked to the membrane's transport properties. Related experiments by Glioza et al.<sup>5</sup> showed that an applied tensile stress could induce an amorphous to crystalline transition in similar collagen films immersed in 6 M KSCN, while simultaneously affecting the film's permeability to tritiated water.

Glioza, Vittoria and Ciferri<sup>6</sup> found that swelling, electrical resistance, streaming potential and water transport changed significantly with bath pH over the pH range 1.5 to 5.0 in solutions of  $10^{-3}$  M  $\text{CaCl}_2$ , as well as  $10^{-2}$  M KCl. While a melting transition between pH 3 and pH 2 was reported at 52 °C, no shrinkage was seen at 25° C. This was consistent with previous X-ray evidence of a crystalline component in rat tail tendon collagen seen even at pH 2.<sup>7</sup> Therefore, the large increases in swelling and dimensional changes that occurred when the pH was lowered from 4 to 2 at 25° C were attributed to Donnan osmotic forces. Titration curves of intact bovine corium collagen show that collagen possesses a positive net fixed charge density for pH<5, negative fixed charge for pH>9, and is essentially neutral (isoelectric) between pH 5 and 9 (for example, see Figure 1).<sup>8</sup> Hence, lowering the pH from 4 to 2 in the above experiments would, in fact, induce a progressively increasing positive fixed charge density and an accompanying Donnan swelling pressure within the membrane. The resulting electrostatic repulsion and osmotic swelling forces generated by collagen fixed charge groups are capable of inducing the observed increase in the volume and changes in the dimensions of the membranes.

Recently, Eisenberg and Grodzinsky<sup>2</sup> used similar collagen membranes and observed that changes in bath pH and NaCl

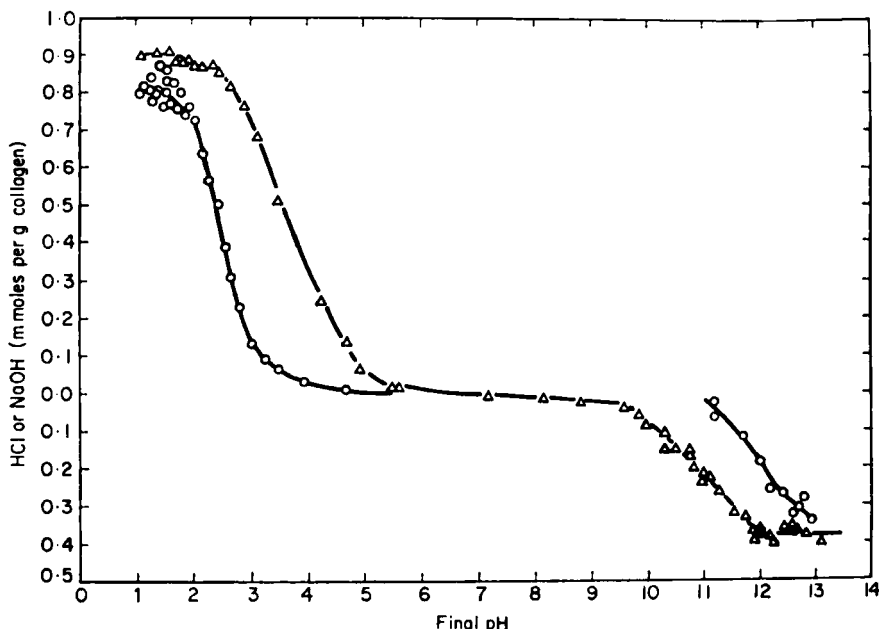


FIGURE 1

Titration curve of intact bovine corium collagen showing the amount of acid or base bound per gram dry collagen vs. bath pH. O, in the absence of salt;  $\Delta$  in the presence of 0.5 M NaCl (Reproduced with permission from Ref. 8).

concentration altered the membrane's permeability to  $^{14}\text{C}$ -sucrose while producing little or no change in the permeability to  $^3\text{H}_2\text{O}$ . These membranes were used previously for studying the electromechanochemical<sup>9</sup> and electrokinetic<sup>10</sup> transduction properties of collagen. Values for the hydraulic permeability, conductance, and electroosmotic coupling coefficient of these membranes obtained in similar electrolyte environments have been reported.<sup>9</sup> These sucrose permeability experiments<sup>2</sup> were part of a larger study of the use of electric fields to control selective changes in membrane permeability, which will be discussed below. Here, it is worthwhile noting that electrostatic repulsion forces

between charged collagen molecules and fibrils (or, equivalently, Donnan swelling forces) appeared to play a dominant role in the observed permeability changes.

### 3. PMAA Membranes

Shatayeva et al.<sup>11</sup> reported that the transport of insulin across membranes of poly(methacrylic acid) (PMAA) was strongly influenced by the ionization state of the membrane as well as the insulin. Furthermore, the existence of a pH gradient across the membrane (pH 2 on one side and pH 7 on the other) appeared to augment the flux of insulin across the membrane. No conclusive explanation of the latter finding was given. However, it was suggested that the pH gradient produced a concomitant gradient in the ionization state of carboxyl groups ( $pK \approx 5.5$ ). This gradient in charge density would generate a "built-in" electric field similar to that at a semiconductor p-n junction. Since insulin is negatively charged above its isoelectric pH=5, the built-in field was thought to produce an additional electrophoretic migration flux of the drug through the membrane, increasing the effective membrane permeability.

An alternative mechanism not discussed by Shatayeva et al is that a gradient in ionization state within a PMAA membrane could produce a gradient in membrane swelling and hydration, which could also affect insulin flux. Figures 2 and 3 show recent measurements<sup>12</sup> of the charge titration and swelling behavior, respectively, of crosslinked PMAA membranes made according to the method of Osada and Saito.<sup>13</sup> These membranes were cast in teflon plates ( $2\frac{7}{8}$  inches in diameter) and were classified by the ratio of the volume of glycerol per 50 ml of 3.3% PMAA solution. Membranes which were .15-.80 mm thick (hydrated at pH 3) were obtained by using 15-30 ml of polymer solution. These data clearly show that as bath pH is increased from pH 2, the increasing concentration of negatively charged carboxyl groups in the membrane is accompanied by a marked increase in water content (from ~50% to over ~80% in the particular PMAA membrane of Figure 3). Further work would have

to be done to distinguish between the possible effects of swelling, Donnan partitioning at the membrane interfaces, and those of the built-in electric field on solute transport in experiments such as those of Shatayeva et al.<sup>11</sup>

#### 4. poly(HEMA) Membranes

Vacik and Kopecek<sup>14</sup> and Kudela et al<sup>15</sup> have studied the properties of yet another variety of hydrophilic gel membranes that is of interest for various medical and separation applications. They used poly(2-hydroxyethyl methacrylate) (HEMA) copolymerized with weakly acidic/basic<sup>14</sup> or strongly acidic<sup>15</sup> groups. For the

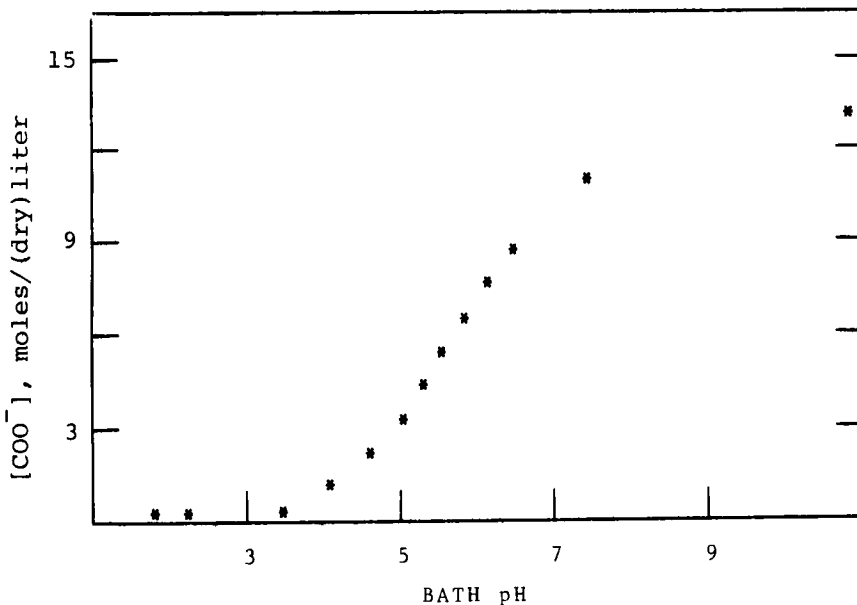


FIGURE 2

Charge density of PMAA membrane vs. bath pH, computed from titration measurement. (Titration behavior was observed to be relatively independent of crosslink density up to 0.35 ml glycerol per 50 ml 3.3% PMAA solution.)

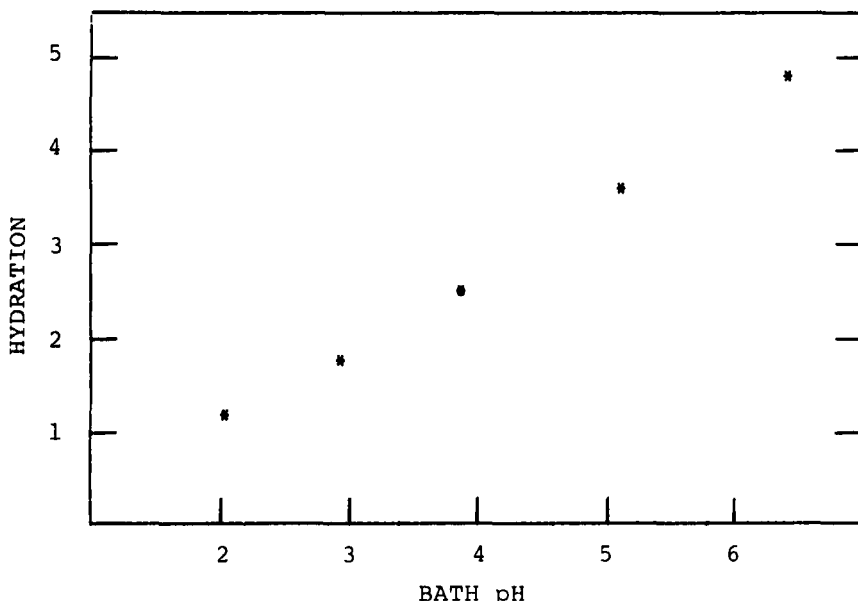


FIGURE 3

Swelling of PMAA membrane vs. bath pH. Membrane composition: 0.25 ml glycerol per 50 ml of 3.3% PMAA solution. (Hydration is defined as volume of membrane water per volume of dry membrane.)

case of weakly acidic/basic groups, the degree of membrane swelling was again altered dramatically by changing the pH of the bathing solution.<sup>14</sup> Membrane resistance decreased as the the content of ionized groups and the hydration increased, a further example of the close link between transport, swelling, and electrochemical properties. With strongly acidic groups, the combination of a high fixed charge density and a high crosslink density (which suppressed swelling) resulted in membranes that showed almost ideal semipermeable behavior. Such behavior is useful for the case of ionic separations.

##### 5. Pore Contraction Induced by Chemical Complexation

Osada and Takeuchi<sup>16</sup> showed that mechanochemical contractions

of a poly(methacrylic acid) (PMAA) film could be induced by reversible complexation with solved poly(ethylene glycol) (PEG). The contractions were ascribed to significant conformational shrinkage of the film's three dimensional network. They hypothesized that if this mechanochemical contraction was developed isometrically, the contractile stresses in the membrane would expand the pores through which water and macromolecular solutes permeate. They proposed this system as an ultrafiltration membrane that could provide improved macromolecular separations.

Figure 4, from Osada and Takeuchi,<sup>16</sup> shows the immediate increase in the water permeability of the membrane that occurred when a small amount of 3000 dalton PEG was added to the water. After studying the effect of varying the molecular weight of the PEG, they concluded that 3000 dalton PEG produced the maximum increase in water permeability and the maximum increase in isotonic contraction<sup>17</sup> and isometric compression<sup>18</sup> of identical PMAA films. The latter finding further suggested that the measured increased in water flux was, in fact, due to expansion of pores.

The potential usefulness of this effect in ultrafiltration was demonstrated by the finding that hemoglobin (64,000 dalton) and albumin (67,000 dalton) solutions permeated the PEG-contracted membrane with the same high rate as pure water, whereas untreated PMAA films were rapidly clogged by these protein solutions. Thus, these mechanochemical membranes showed both high water permeability and good retention of water soluble solutes.

We have thus far considered changes in membrane transport and separation properties that are linked with swelling and electrostatic effects that can be controlled by the chemical environment of the membrane. Applied electric fields can also be harnessed to effect such precise modulation of the local chemical environment in the neighborhood of membrane macromolecules. This is one of the bases for systems involving electric field control of membrane permeability. Thus, the purpose of the electric field is to produce and smoothly control the type of change in water or solute permeability such as that shown in Figure 4. Furthermore,

the application of electric field could be feedback-controlled by the use of appropriate sensors.

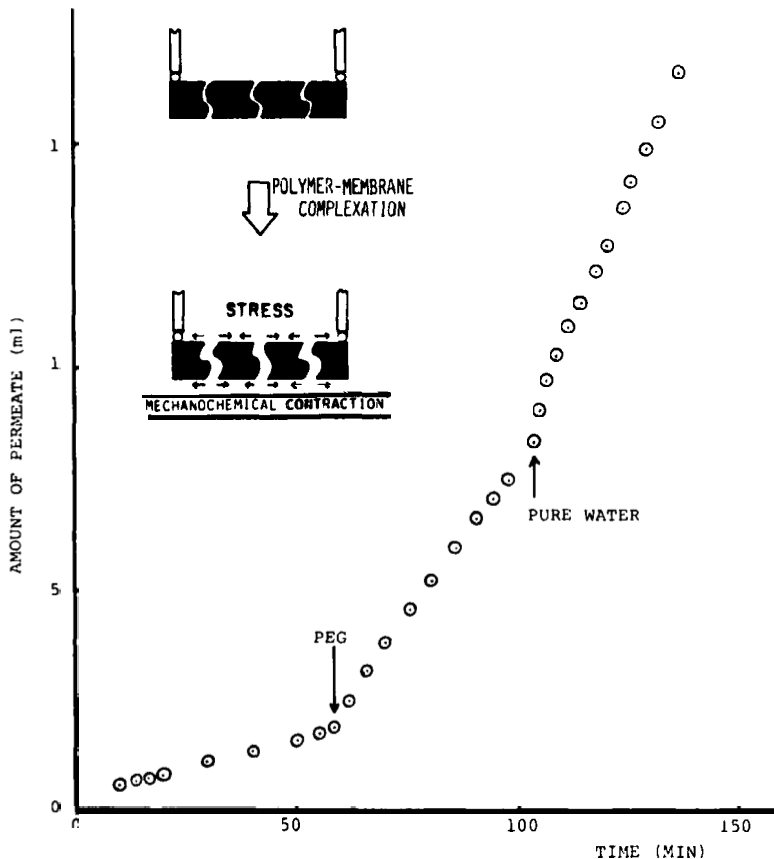


FIGURE 4

Effect of mechanochemical contraction of PMAA membrane on water permeation. PMAA membrane:  $3.4 \text{ cm}^2$  area,  $30 \mu\text{m}$  thickness. PEG added: mol wt = 3000,  $5.8 \times 10^{-2}$  mol/liter solution, transmembrane pressure:  $0.2 \text{ kg/cm}^2$ . Insert: schematic representation of mechanochemical contraction of PMAA membrane by polymer-membrane complexation (reproduced with permission from Ref. 16).

## 6. Drug Delivery

An increasingly important application of these fundamental properties of charged membranes and polymers is in the area of swelling-controlled drug delivery systems. In a review of biomaterials in controlled drug delivery systems, Langer and Peppas<sup>19</sup> identified swelling-controlled systems as one of four main classes of polymeric release mechanisms. In one such system, the glassy/rubbery phase transition of polymers is employed as a means of changing the release rate of an embedded drug. Drug molecules are first dispersed in a polymer matrix or capsule. After the solvent has evaporated from the polymer matrix, drug will not diffuse through the resulting glassy polymer. When the polymer is immersed in water, a glassy-to-rubber phase transition occurs with concomitant swelling, enabling the drug to dissolve and diffuse out of the polymer matrix. The release rate of the drug is affected by the kinetics of swelling of the polymer, which evolves as dissolution and diffusion of drug take place. The occurrence of Fickian versus anomalous diffusion is characterized by the dimensionless Deborah number,  $D_e$ , defined as the ratio of the polymer matrix stress relaxation time to the diffusion time of the macromolecule.<sup>19</sup>

When the polymer contains ionizable charge groups, electrostatic effects may affect drug release in two ways. As mentioned above, swelling of such a polymer may be greatly enhanced by electrostatic repulsion forces, thereby altering polymer permeability to neutral or charged drug molecules. If the drug itself is charged, then additional electrostatic interactions between drug and polymer can affect drug transport.

Kost et al.<sup>20</sup> and Horbett et al.<sup>21</sup> have described a polymeric membrane system that may have important applications for glucose detection and for controlled delivery of insulin at rates dependent on external glucose concentration. Glucose oxidase is immobilized within a HEMA-based membrane that also contains amine groups bound to its network. Glucose entering the membrane is catalyzed to gluconic acid by the bound enzyme, which lowers the intramembrane

pH and thereby increases the membrane's positive fixed charge density. This results in increased swelling of the membrane by 16-18%<sup>21</sup> when bath pH reaches  $\approx 3$ . In this swollen state, the membranes were found to be more permeable to small solutes such as  $^{14}\text{C}$  ethylene glycol and iodide by factors of 1.3 and 2.1, respectively.<sup>20</sup> However, the permeability of these membranes to insulin was below the sensitivity range of the assay ( $10^{-9}$   $\text{cm}^2/\text{sec}$ ). This was ascribed to the repulsive interaction (Donnan partitioning) between membrane and insulin positive charge groups at low pH.<sup>20</sup> Figure 5 shows the change in permeability of these

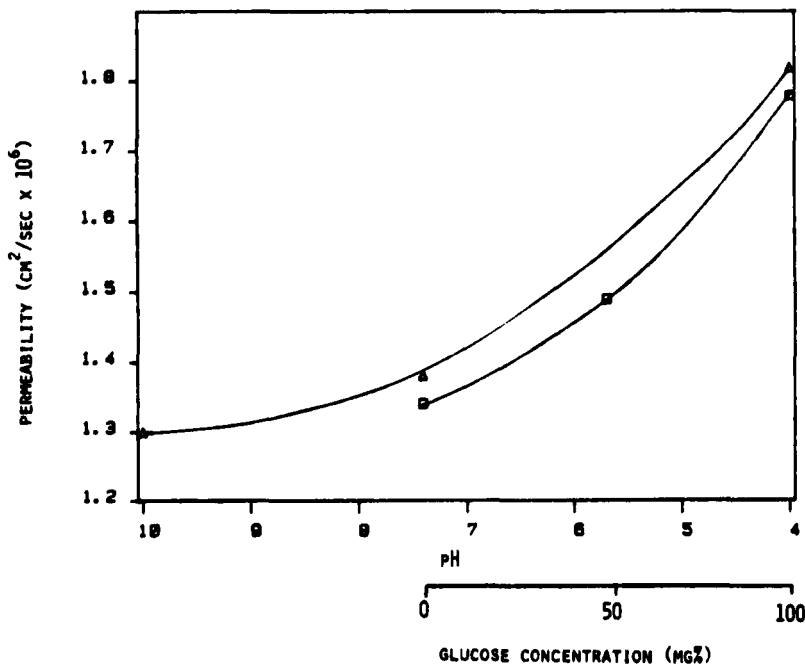


FIGURE 5

The effect of pH and glucose concentration on the permeability of ethylene glycol. The two curves correspond to two different membrane formulations (reproduced with permission from Ref. 20).

glucose-sensitive membranes to ethylene glycol in response to changes in imposed external bath pH as well as to changes in the glucose concentration of phosphate buffered saline.<sup>20</sup>

Another drug release system based on pH-control has been described by Bala and Vasudevan.<sup>22</sup> They studied the microencapsulation and cumulative release of secretin from acryloyl-chloride lysine capsules, and observed that release was linear with time over several days (zero-order kinetics) but depended markedly on the pH of the buffer which contained the capsules. Since secretin release in-vivo is pH sensitive (i.e., any time the pH of the duodenum falls below ~4),<sup>22</sup> this microencapsulation system could mimic the conditions of natural delivery. The mechanism of release from the capsules was not completely understood, but it was suggested that polymer dissolution occurred at a rate dependent on pH.<sup>22</sup> Swelling and other possible pH-dependent mechanisms were not discussed.

### III. HINTS FROM BIOLOGICAL SYSTEMS

Regulation of membrane permeability has long been studied in a wide variety of biological cell and tissue preparations. The possibility that changes in membrane microstructure can modulate membrane permeability has received much attention. Such changes in microstructure are produced both chemically and electrically.

For example, the structure and packing density of charged lipid bilayers can be changed by slight alterations in electrolyte pH or the concentration of monovalent and divalent cations.<sup>23</sup> Such phase changes have been ascribed to lateral electrostatic repulsion forces in the plane of the bilayer, and can result in modification of bilayer adsorption and chemical binding properties.<sup>23</sup>

Wieth et al.<sup>24</sup> summarized the work of several groups showing the effect of pH-induced morphological changes in red cell membrane that can significantly alter membrane permeability. A seven-fold increase in chloride self exchange flux occurred across resealed

human erythrocyte ghosts when bath pH was lowered from 5.1 to  $\approx 4.8$ .<sup>24</sup> This phenomenon was associated with aggregation of cytoskeleton proteins having an isoelectric point at pH 5. Such aggregation is thought to lead to formation of channels permitting transport of small hydrophilic molecules and ions, but impermeable to larger molecules such as inulin.<sup>24</sup> These observations suggested that electrostatic forces at physiological pH (nonisoelectric conditions for cytoskeleton molecules) are essential in the maintenance of normal membrane microstructure and permeability.

With regard to biologic electric field control, nerve and muscle membranes provide the most often cited examples of the coupling of electrical signals to membrane transport properties.<sup>25</sup> The possibility that a change in the conformation of protein constituents in such excitable membranes could lead to changes in ion permeability has been linked to the transmembrane electrical potential. Schmitt and Davison proposed a model<sup>26</sup> in which proteins are induced to change their shape in response to transmembrane fields or ions driven electrophoretically across the membrane. This would lead to a series of events thought to change the structure of specific pores that mediate the passage of  $\text{Na}^+$  and  $\text{K}^+$  ions. In a related hypothesis, Goldman<sup>27</sup> suggested that transmembrane electric fields in excitable membranes could change the intramembrane ionic strength in the vicinity of membrane proteins, causing a change in protein conformation, and thereby changing the membrane's permeability. Blank<sup>28</sup> has emphasized the important role of the electrical double layers at the membrane-solution interfaces. The link between ion concentration changes and current flow that exists at such interfaces in physiological membranes has been examined in the context of Blank's "surface compartment model".<sup>28</sup>

#### IV. ELECTRIC FIELD CONTROL OF MEMBRANE TRANSPORT AND PERMEABILITY

##### 1. Electroactive Polymer Membranes and Coated Electrodes

Recent studies have described novel phenomena and device applications based on the use of special polymer films that are

confined to electrode surfaces. Redox reactions within the polymer can be catalyzed at such electrodes for applications including electrochemical analysis of trace components,<sup>29</sup> electrochemical display devices,<sup>30</sup> the creation of anion selective surface films,<sup>31</sup> controlled release of dopamine (a neurotransmitter) from a polymer film,<sup>32</sup> and gating of ion transport across polymer films.<sup>33,34</sup>

Of particular relevance to this review, Burgmayer and Murray<sup>33,34</sup> have studied an ion gate membrane in which an electrochemical reaction within the membrane controlled by an applied voltage causes a change in the permeation of certain ions across the membrane. They electropolymerized a 10 $\mu$ m cationic poly(pyrrole) redox film onto a porous gold grid (5 $\mu$ m pore size). Application of -0.9 V to the embedded grid with respect to a standard calomel electrode in the bath reduced the film from a poly-cationic state to a neutral state. This increased the resistive part of the membrane impedance at 2 Hz from about 20 $\Omega$  to 13k $\Omega$  with a time constant of about 30 min.<sup>31</sup> Reoxidation of the membrane (grid at +0.5 V vs. SCE) reduced membrane resistance to its initial low state at a more rapid rate. Independent measurements<sup>34</sup> showed a two-order-of-magnitude decrease in the flux of Cl<sup>-</sup> ions across a membrane which separated 1.0M KCl and 1.0M KNO<sub>3</sub> solutions when the membrane was cycled from the oxidized to the reduced state. Changes in membrane ultrastructure or swelling were not reported.

## 2. Electrokinetics in Ultrafiltration

Pasechnik et al<sup>35</sup> applied a dc current density of 0.01 to 5.0 ma/cm<sup>2</sup> via platinum electrodes situated in the adjacent baths, during a protein ultrafiltration experiment. They observed an increase in hydraulic permeability when the current was applied. The transport of protein per volume of fluid increased in response to the applied field depending on the size of the protein. They concluded from their data that electroosmosis was not significant, and ascribed their result to an unknown electrohydrodynamic effect which increased the pore size of the membrane. Since this effect

was reported to be independent of current polarity, it is probably not related to electrophoretic particle migration away from the concentration polarization layer, a phenomenon described by Henry et al.<sup>36</sup> and Radovich and Sparks.<sup>37</sup> In addition, pH changes caused by electrolysis were not controlled by Pasechnik et al, which could affect both membrane and solutes.

Henry et al.<sup>36</sup> modeled a crossflow/electrofiltration process designed to improve rates of filtration through various media. The process combined the mechanisms of electrophoretic particle transport in the filter medium and the liquid film adjacent to the medium, electroosmosis in the medium, and transport induced by high circulation velocity. The model showed that film resistance could be controlled in part by the applied field. Radovich and Sparks<sup>37</sup> observed that an applied field could control the build up of retained macrosolutes at a membrane surface, and thereby increase ultrafiltration flux by 75% to 500%. Experiments were conducted in the pH range 4.7 to 8.1 using Amicon Diaflo membranes and solutions of bovine albumin,  $\gamma$ -globulin, and fibrinogen. They ascribed this effect to solute electrophoretic migration in the gel polarization layer, and found independently that electroosmosis in the gel layer was negligible.

Given that gradients in pH and ionic strength will exist across such a gel-polarization layer at the membrane surface during ultrafiltration, it is possible that an applied electric field may alter the characteristics of the gel by additional mechanisms. For example, an applied field can change the pH and ionic strength within the gel layer (see next section) which may affect the permeability of the layer. Radovich and Sparks<sup>37</sup> found that imposed changes in the pH or ionic strength of the protein solutions had little effect on ultrafiltration flux, compared to turning on the field. However, we will see below that changes in pH and/or ionic strength controlled by an applied field can have important effects on the transport properties of natural and polymeric-gel membranes.

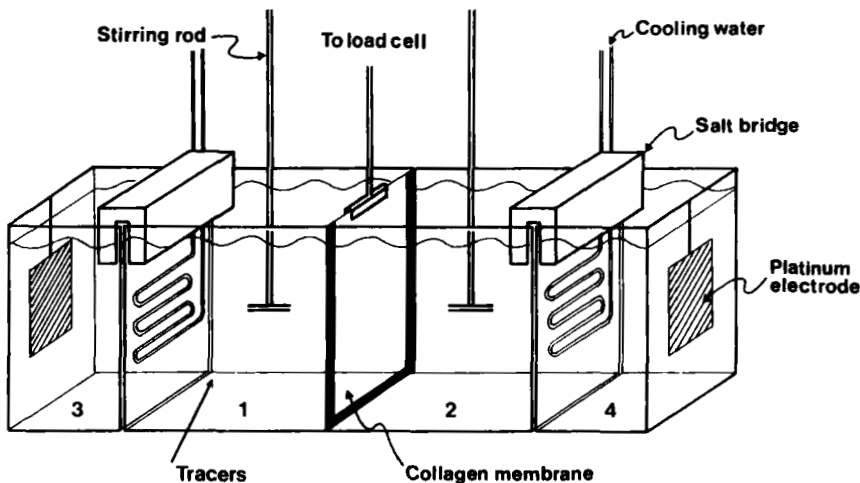


FIGURE 6

Schematic of transport cell for measurement of tracer flux and membrane isometric tensile force. Membrane chambers 1 and 2 are connected to electrode chambers 3 and 4 by polyacrylamide-gel salt bridges (reproduced with permission from Ref. 2).

### 3. Electrodiffusion: Control of Intramembrane Concentration Profiles and Membrane Molecular Interaction Forces

When an electric field is applied across a membrane that supports a gradient in the concentration of mobile ions, the field will affect the intramembrane concentration profiles of these ions by the process of electrodiffusion.<sup>38</sup> In deformable, charged membranes, changes in intramembrane ionic strength or pH can cause dramatic changes in membrane swelling and rheological properties, as we have reviewed above. An applied electric field can provide the means for fast, localized control of intramembrane ionic strength and pH via the mechanism of electrodiffusion. The possibility that the field can thereby control membrane mechanical properties and solute permeability has been investigated in a

series of experiments with membranes of collagen<sup>2,9,39-41</sup> and, more recently, poly(methacrylic acid).<sup>12,42</sup>

Bovine hide corium collagen membranes were placed in one of several transport cells similar to that of Figure 6. In one series of experiments, a membrane separated electrolyte baths of differing NaCl concentration (0.0004 M/0.04 M) but identical pH=2.8 (HCl).<sup>9</sup> Each such membrane was clamped by the cell at the bottom and sides, while the top was clamped to a rod connected to a load cell. This enabled continuous monitoring of the membrane's isometric tensile stress in order to obtain a measure of the changes in the mechanical or swelling properties of the membrane that were induced by the applied field.

When a sinusoidal electric field was applied across the membrane, a sinusoidal tensile force was observed to occur at the same frequency. The data of Figure 7 show the amplitude and the phase of the measured force with respect to the applied field over a three decade frequency range. With hydrated membrane thickness approximately 160  $\mu\text{m}$ , the maximum applied current density of 2.3 mA/cm<sup>2</sup> in Figure 7 corresponded to a transmembrane potential of about 19 mV and an electric field of 1.15 V/cm.

It was hypothesized that the tensile force was produced by anisotropic swelling of the membrane predominantly in its thickness direction in response to a field-induced change in intramembrane ionic strength. Such a change in ionic strength would modulate double layer repulsion forces between the charged collagen molecules and/or fibrils of the membrane, which are randomly oriented in the plane of the membrane. Thus, an increase in intermolecular and interfibrillar forces would increase swelling predominantly in the thickness direction. This would tend to cause contraction along the plane of the membrane and a concomitant increase in measured tensile force in the configuration of Figure 6. (The importance of these mechanical effects on membrane permeability is discussed below).

To test this hypothesis, a theoretical model was formulated for the change in salt concentration induced by the applied

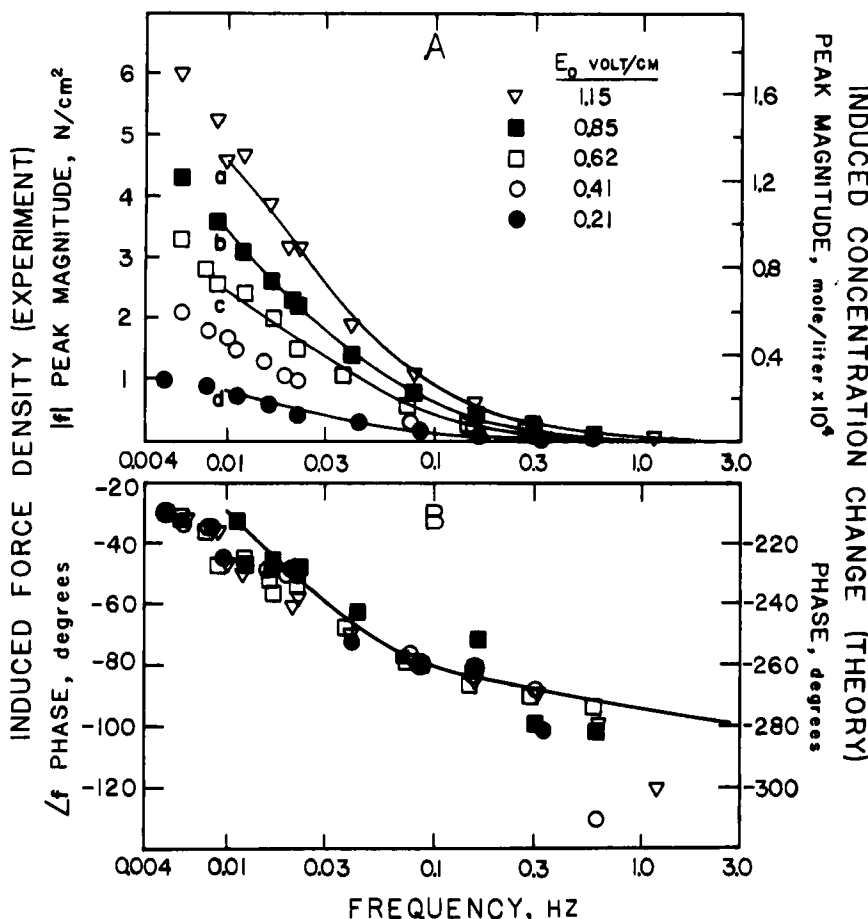


FIGURE 7

(A) Variation of the peak magnitude of the electrically induced change in isometric force density with frequency. The data correspond to five electric field amplitudes  $E_0$ . The force density is the total force normalized to dry cross-sectional area. Solid lines correspond to theoretical calculations of the electrically induced changes in intramembrane NaCl concentration, with  $E_0$  values (V/cm) of a, 1.2; b, 0.88; c, 0.65; and d, 0.215, respectively. A value of  $(\delta^2/\pi^2 D_+) = 9.0$  sec was used for all theoretical curves.

(B) Phase of  $f$  with respect to the applied  $E_0 \sin(2\pi t)$ , versus frequency. Data correspond to the same  $E_0$  amplitudes as (A). Solid line corresponds to theory with  $(\delta^2/\pi^2 D_+) = 9.0$  sec (reproduced with permission from Ref. 9).

electric field within the positively charged membrane. The change in salt concentration was dominated by NaCl in this experiment,<sup>9,39</sup> and was predicted to a good approximation by focusing on the electrodiffusion equation for the Na<sup>+</sup> cation (see APPENDIX):

$$\frac{D\bar{c}_{Na}}{Dt} = D_{Na} \frac{\partial^2 \bar{c}_{Na}}{\partial x^2} - \bar{u}_{Na} E_x(t) \left[ 1 - \frac{L_{12}\delta}{\bar{u}_{Na}} \right] \frac{\partial \bar{c}_{Na}}{\partial x} \quad (1)$$

where  $\bar{c}_{Na}$ ,  $D_{Na}$ , and  $\bar{u}_{Na}$  are the intramembrane Na<sup>+</sup> concentration, diffusivity, and mobility, respectively,  $L_{12}$  the electroosmotic coefficient of the membrane,  $\delta$  the membrane thickness,  $E_x(t)$  the applied unidirectional electric field, and  $D/Dt$  the convective derivative (see APPENDIX).

Eq. (1) can be solved subject to boundary conditions on concentration at the two edges of the membrane and initial conditions. The boundary concentrations were determined from the time-invariant external bath concentrations and Donnan partitioning laws at the membrane interfaces. For steady (dc) applied fields, the solution to (1) with  $(Dc_+/Dt)=0$  is

$$\bar{c}_+(x) = \frac{\exp\left[\frac{\alpha}{2} \frac{E(x-\delta)}{V_T}\right] \bar{c}_+(\delta^-) \sinh\left[\frac{\alpha}{2} \frac{Ex}{V_T}\right]}{\sinh\left[\frac{\alpha}{2} \frac{E\delta}{V_T}\right]} - \frac{\exp\left[\frac{\alpha}{2} \frac{Ex}{V_T}\right] \bar{c}_+(0^+) \sinh\left[\frac{\alpha}{2} \frac{E(x-\delta)}{V_T}\right]}{\sinh\left[\frac{\alpha}{2} \frac{E\delta}{V_T}\right]} \quad (2)$$

where  $V_T$  is the thermal voltage  $RT/F$  ( $\approx 25$  mv at  $25$  °C) and  $\alpha \equiv (1 - L_{12}\delta/\bar{u}_+)$ .

Figure 8 shows steady state Na<sup>+</sup> cation concentration profiles calculated from Eq. (2) for transmembrane potential drop  $E\delta$  between zero and  $8RT/F$ , where  $\delta$  is membrane thickness. Since electroneutrality must be satisfied, an equal change in

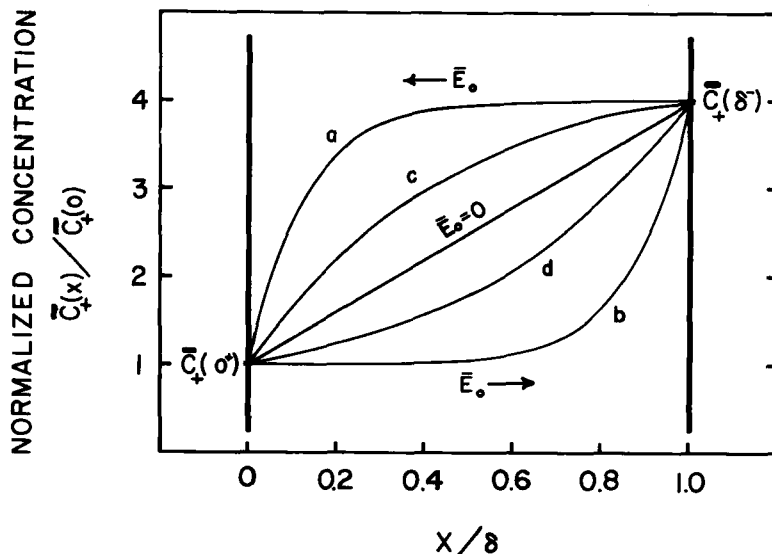


FIGURE 8

Calculated normalized perturbation concentration inside a membrane of thickness  $\delta$  for values of applied electric field  $\bar{E}_0$ ; positive fixed charge density.

a,b  $|\bar{E}_0| = 200$  mv; c,d  $|\bar{E}_0| = 50$  mv;

a,c,  $\bar{E}_0 < 0$ ; b,d,  $\bar{E}_0 > 0$ ;

(Reproduced with permission from Ref. 39)

intramembrane counterion ( $\text{Cl}^-$ ) concentration must also occur. (We note that in actuality, a gradient in concentration of  $\text{NaCl}$  will produce a steady state diffusion potential across the membrane, since  $\bar{D}_{\text{Na}} \neq \bar{D}_{\text{Cl}}$ . Thus, ion concentration profiles will be slightly curved even in the absence of an applied field. However, the curves of Figure 8 can still be used to judge the change in concentration that would be produced by an applied field).

Based on calculations such as those of Figure 8, theoretical curves of the amplitude and phase of the intramembrane change in  $\text{NaCl}$  concentration for the conditions of Figure 7 were computed, and are shown in Figure 7. The only adjustable parameter in the

theoretical phase angle is the cation diffusivity.<sup>9</sup> For reasonable values of this parameter, the phase of the concentration change fit well to the phase of the measured force. This provided direct evidence that the kinetics of the mechanical property change matched that of the field-induced concentration change and, hence, evidence that electrodiffusion was the predominant mechanism.<sup>9</sup>

Experiments were also performed using stepwise transient<sup>39,2</sup> applied fields, enabling further examination of the kinetics underlying the field-induced changes in mechanical properties. For the case of an NaCl gradient across the membrane, the time constant for the observed change in force agreed well with the electrodiffusion time<sup>43</sup>:

$$\tau_{ed} = \frac{\delta^2}{\pi^2 \bar{D}_+} \left( 1 + \left[ \frac{E\delta}{2\pi(RT/F)} \right]^2 \right)^{-1} \quad (3)$$

For the case of a pH gradient in the acidic range across the membrane (with equal NaCl concentrations on both sides), H<sup>+</sup> is a cation. An applied field will alter the intramembrane pH since the H<sup>+</sup> profile also satisfies an electrodiffusion equation of the form (1), but with an additional term associated with the binding of H<sup>+</sup> ions to ionized carboxyl groups within the collagen membrane. Changes in intramembrane pH alter the collagen fixed charge density (Figure 1) and, hence, will also produce changes in isometric tensile force.<sup>2</sup> The time constant for observed changes in force produced by an electric field with such a pH gradient was much longer than that predicted by Eq. (3). Rather, the time constant was on the order of the diffusion-limited chemical reaction time previously found when the pH was changed directly by titration with HCl<sup>40</sup>:

$$\tau_{dr} = \frac{\delta^2}{\pi^2 \bar{D}_H} \left[ 1 + \frac{Kn}{(K+\bar{c}^0)^2} \right] \quad (4)$$

where  $\bar{D}_H$  and  $\bar{c}^0$  are the intramembrane diffusivity and equilibrium concentration of H<sup>+</sup> ions, and K and n<sub>-</sub> are the intrinsic

dissociation constant and molar concentration of the collagen carboxyl groups.

Eq. (4) shows that that transport of  $H^+$  within the membrane can be slowed by binding to charge groups; hence,  $\tau_{dr}$  can be several orders of magnitude longer than a simple diffusion time when many binding sites are available ( $\bar{c} \ll K$  or, equivalently,  $pH \gg pK$ ). This would hold whether the pH was changed by electrodiffusion or by direct titration.

The observed time constants for changes in isometric tensile force in collagen were rate limited by chemical transport processes. This suggests that mechanical swelling occurred at least as rapidly as chemical diffusion (NaCl) or diffusion-reaction (HCl).<sup>44</sup> With certain polyelectrolyte gels this may not be the case, as network swelling may be rate-limiting.<sup>44</sup>

The ability of an applied electric field to alter intramembrane concentration profiles of charged solutes has recently been demonstrated in a very different electrodiffusion system. Valleton,<sup>45</sup> Valleton et al.,<sup>46</sup> and Selegny et al.<sup>47</sup> have studied membranes containing immobilized enzymes and the ability of ac and dc applied fields to mediate enzyme reactions by modulating the intramembrane distribution of  $H^+$  ions, ionic substrates or cofactors. Variation in the concentration of one or more of these "mediators" thereby induces variations in enzyme activity. Theoretical models were derived for a wide variety of enzyme/mediator systems in which a membrane separated baths having equal concentration of a neutral supporting electrolyte, but different concentration of an ionic mediator.

One experiment designed to demonstrate the effect of the field utilized a gradient in D-glucose-6-phosphate tagged with  $^{14}C$  across a 5%, 5mm thick agarose gel membrane, and 0.01 M KCl as the supporting electrolyte.<sup>45,46</sup> After steady state profiles of the  $G_6P^{--}$  were established with and without an applied field, a deep freezing microtome was used to section the membrane in 300  $\mu m$  slices. The radioactivity of each slice gave an approximate measure of the solute concentration profile. Figure 9 shows that in the

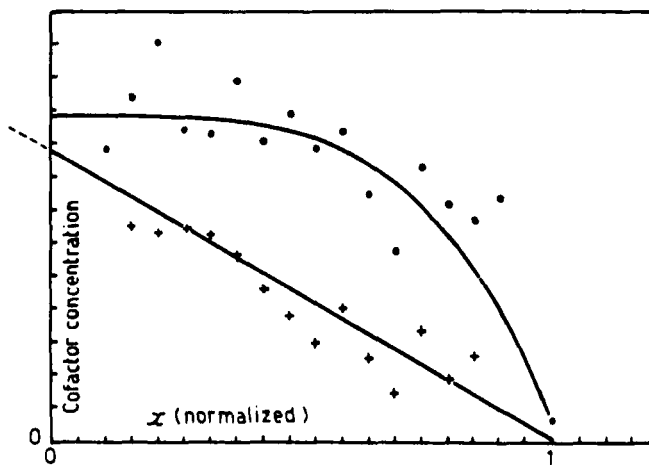


FIGURE 9

Intramembrane concentration profiles of activator, experimentally obtained with asymmetric boundary conditions; the ion used was labeled with  $^{14}\text{C}$ ; (+) diffusion regime, (0) electrodiffusion regime (reproduced with permission from Ref. 47).

absence of an applied field, the  $\text{G}_6\text{P}^{4-}$  solute was distributed linearly across the membrane in the steady state, as predicted by simple diffusion analysis. With the field, the solute concentration was bowed in a fashion that agreed with a polynomial approximation to an analytical expression similar to Eq. (2).<sup>46</sup> The similarity between the curves of Figure 9 and those of Figure 8 is immediately apparent.

#### 4. Electrodiffusion: Control of Membrane Permeability

The results of collagen membrane experiments such as those described above, which involved field-induced changes in isometric stress,<sup>2,41</sup> suggested that membrane pore size and permeability might be affected by the same electrodiffusion mechanism. That is, modulation of intramembrane pH or ionic strength would alter electrostatic repulsion forces between membrane molecules and

fibrils. The distances between these structural elements are determined by a balance between such repulsive forces and the mechanical constraints of chemical crosslinks and physical entanglement. These separation distances constitute one of the parameters of membrane ultrastructure that determines the sieving and transport properties of the membrane.

In order to test this hypothesis, double tracer flux experiments using the neutral solutes  $^3\text{H}_2\text{O}$  and  $^{14}\text{C}$ -sucrose were performed using these same collagen membranes. The results demonstrated that the field could selectively change the membrane's permeability to  $^{14}\text{C}$ -sucrose, while permeability to  $^3\text{H}_2\text{O}$  was minimally affected. This behavior was elicited when the membrane supported a gradient in either pH or NaCl concentration. Figure 10 shows the concentration of tracers versus time for one of a series of such experiments which showed an average change in sucrose permeability of 26% with negligible change in  $^3\text{H}_2\text{O}$  permeability (see Ref. 2 for details). The trends of the response have been clearly established. Additional tests showed that neither electroosmosis nor a simple electrophoretic bowing of the membrane had a significant effect on transport in these experiments.<sup>2,41</sup> It was concluded that changes in membrane microstructure and/or hydration induced by the mechanism of electrodiffusion were of primary importance.

Double tracer experiments such as Figure 10 enabled us to compare changes in the flux of small solutes ( $^3\text{H}_2\text{O}$ ) with larger molecular weight solutes. Small neutral solutes and hydrated ions are known to be freely exchangeable with the entire collagen membrane volume, and therefore small changes in intermolecular spacing would not be expected to alter the transport of  $^3\text{H}_2\text{O}$ . However, small changes in membrane microstructure can have a significant effect on diffusivity of larger solutes whose size is not negligible compared to the estimated 1-3 nm pore radius of the membrane. This is motivated by the well known phenomenon of restricted diffusion.<sup>48</sup> This suggests that optimal use of this mechanism for modulating membrane permeability will depend on successfully matching the membrane's morphology and ultrastructure

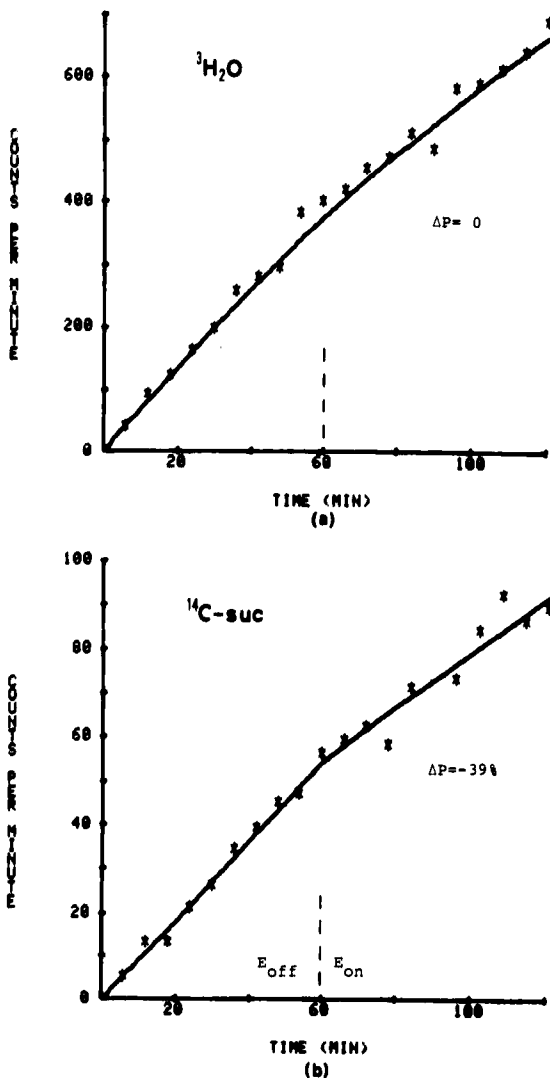


FIGURE 10

$^3\text{H}_2\text{O}$  and  $^{14}\text{C}$ -sucrose concentration (DPM) in the cold chamber vs. time. The solid curves are best fit spline functions used to compute tracer flux before and after application of the electric field at  $t = 60$  min.

to the size of the solutes of interest in a given separation or delivery process.

#### V. REAL TIME MEASUREMENT OF MEMBRANE PERMEABILITY CHANGES USING FLUORESCENT PROBES

While the radiotracer/electrodiffusion experiments described thus far showed that modification of membrane permeability can be achieved by this method, the magnitude of the observed changes was small. Therefore, we have begun to explore other membrane materials and membrane/solute combinations. In addition, we have begun to use techniques based on fluorescence methods which enable measurement of membrane transport in real time and therefore will speed our ability to optimize membrane/solute pairs. The permeability of the membranes to certain fluorescent dyes has recently been measured using an apparatus shown schematically in Figure 11. Experiments completed thus far show that the permeability of PMAA and collagen membranes to these dyes can be changed by factors of approximately 20-100 by modification of the bath pH. This is to be compared with factors of 1.5 or less found in the radiotracer studies.<sup>1,40</sup> The magnitude of the permeability change again depends on the relationship between the solute size and the effective pore size of the membrane. It is therefore expected that electric field modulation of membrane permeability in these same systems can be proportionately higher than that of Figure 10, for example.

Transport experiments in which bath pH was abruptly changed demonstrated the ability of the fluorometer to resolve permeability changes in real time. In Figure 12a and b,  $T_0$  denotes the time at which the bath pH was changed by the addition of a small volume of concentrated acid or base. In each case, the flux of dye through the membrane increased by a factor of about 20.

Figure 12a was obtained using a negative cyanine dye ( $\text{diI-C}_3\text{SO}_3^--(5)$ )<sup>49</sup> as the solute probe and a collagen membrane. When the bath pH was changed from 5 to 3, the initially uncharged membrane attained a net fixed positive charge density (see Figure

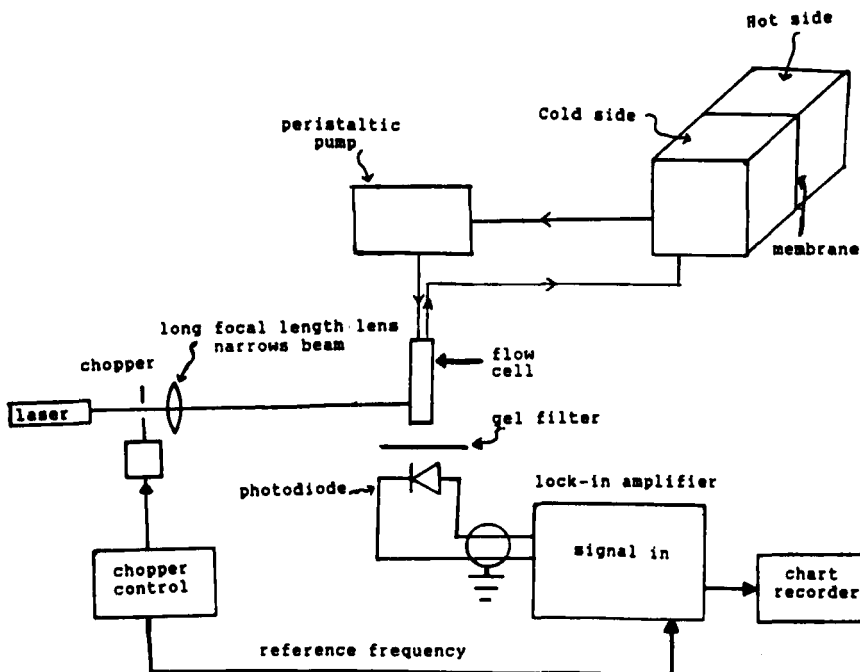


FIGURE 11

Schematic of apparatus for measurement of fluorescent-dye transport across membranes.

1). The transient decrease in fluorescence intensity immediately following  $T_0$  in Figure 12a may be attributed to the Donnan partitioning of the negatively charged dye into the membrane. This occurred as soon as the membrane began to acquire positive charge, thereby decreasing the dye concentration in the baths. This transient was followed by an increased transmembrane flux of dye in the steady state, as seen by the slope of the fluorescence versus time data. The increase in dye flux could be caused by a change in effective pore radius (for example, a change in hydration or interstitial spacing), or by the increased intramembrane dye concentration gradient that accompanied the change in Donnan partitioning.

Figure 12b shows the result of a similar experiment using the same negative dye together with a PMAA membrane. The PMAA was transformed from an uncharged to a negatively charged state when the bath pH was increased from 3 to 4.35 by addition of KOH at time  $T_0$ . The observed increase in the steady state flux is noteworthy since this increase occurred despite Donnan exclusion of the dye and the associated decrease in the intramembrane dye concentration gradient. Thus, the observed permeability increase must be due to an increase in effective pore size. The immediate transient that followed  $T_0$  in Figure 12b was also consistent with Donnan expulsion of the negative dye from the membrane as the fixed negative charge density increased, and is the complement to the transient that followed  $T_0$  in Figure 12a.

The data of Figure 13 shows that changes in bath pH can be used to reversibly open and close a PMAA membrane to the transport of dye. In this experiment, the PMAA membrane was more heavily

#### TRANSPORT OF FLUORESCENT PROBE

MEMBRANE: COLLAGEN

DYE: CYANINE  $\ominus$

SLOPE INCREASES BY  $\times 22$

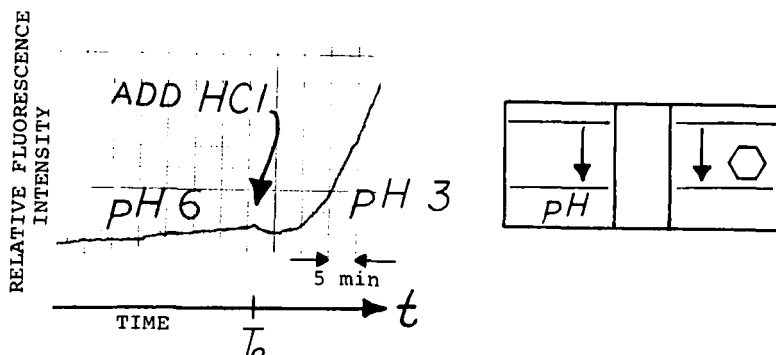


FIGURE 12a

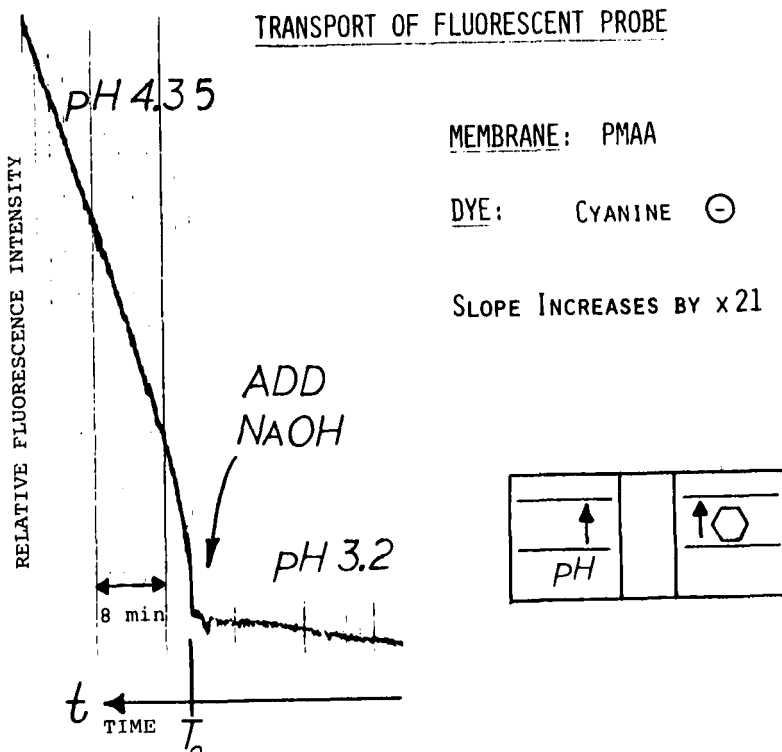


FIGURE 12b

crosslinked than that of Figure 12b, so that virtually no dye could pass at pH 3.5. However, when the pH of the external baths was raised to a pH of about 5.5, the cyanine dye was able to diffuse through the membrane. Once again, the negatively charged dye was a co-ion. Hence, the increased dye transport at high pH must be due to swelling of the membrane (which would increase the effective pore size).

A fluorescein labeled dextran (MW 4000) was also used as a solute for transport experiments. A comparison of the permeability of our PMAA membranes to the dextran versus the cyanine dye for three different membrane crosslink densities is given in Table I.

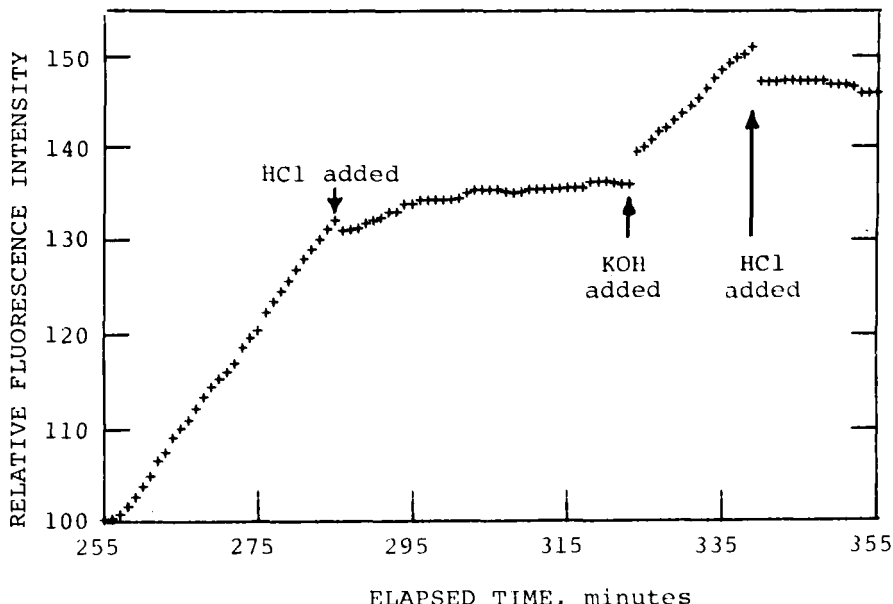


FIGURE 13

Effect of pH changes ( $\sim 3.5$  to  $\sim 6.0$ ) on the transport of  $\text{dil-C}_3\text{SO}_3^-$ -(5) across a PMAA membrane (0.35 ml glycerol per 50 ml 3.3% PMAA solution). Although bath pH had not reached steady state before the next addition of acid or base (due to the slowness of titration), the "on-off" behaviour of membrane permeability is demonstrated.

Note that in all cases, permeability of the dextran was less than that of the cyanine, all other conditions being equal. We also see how the magnitude of the permeability change depends critically on matching membrane characteristics (such as crosslink density and fixed charge density) to solute characteristics (such as size). Because of the pH sensitivity of fluorescein, the kinetics of the permeability changes were masked by changes in bath pH as the membrane fixed charge titrated to steady state. Nevertheless, steady state permeabilities could still be resolved. In some cases, no transport was observed for the duration  $T$  of a given experiment.

TABLE I

	Solute Permeability ( $10^6$ cm/sec)			pH
	MEMBRANE COMPOSITION (ml glycerol per 50 ml 3.3% PMAA solution)			
DYE	0.20	0.25	0.35	
FITC- Dextran	2.0	<0.87	<0.11	pH≈3.7
	2.3-4.6	1.2	0.42	pH≈5.5
dI <sub>I</sub> -C <sub>3</sub> SO <sub>3</sub> <sup>-</sup> (5)	-	3.8	<0.40	pH≈3.7
	-	11.9	0.96	pH≈5.5

The membrane thickness at pH 3.5 was:

0.5 mm for the 0.20 membranes.

0.8 mm for the 0.25 membranes.

0.15 mm for the 0.35 membranes.

Membrane crosslink density increases with glycerol content.

While such data suggests negligible membrane permeability to solute, the possibility exists that  $T$  corresponds to the diffusion time lag beyond which increased solute concentration on the downstream side would occur. This interpretation would correspond to an upper bound on permeability equal to  $\frac{50}{6T} \delta$ , which has been indicated in Table I by the inequality notation.

Addition of a neutral salt to the bath may alter the hydration of a membrane either by increased screening (which will always reduce the hydration), or by altering the intramembrane pH (which will always increase the membrane fixed charge density). For the case of a PMAA membrane in baths of pH 5-6, altering the bath KCl concentration from 0.001 M to 0.1 M did not significantly change the permeability of the membrane to dI<sub>I</sub>-C<sub>3</sub>SO<sub>3</sub><sup>-</sup>(5), although

transients similar to those observed in Figure 12 were seen to be consistent with Donnan partitioning. This result may be due to the highly nonlinear relationship between swelling and permeability when stearic effects are involved. Alternatively, the change in bath salt concentration may have altered intramembrane pH (hence, intramembrane fixed charge) so as to counteract the shielding effect of the salt. A calculation of intramembrane pH versus bath pH for several concentrations of a mono:monovalent neutral salt in the region of interest (Figure 14) shows this interrelationship.

Figure 15 shows an example of an experiment in which the change in intramembrane fixed charge density caused by adding KCl

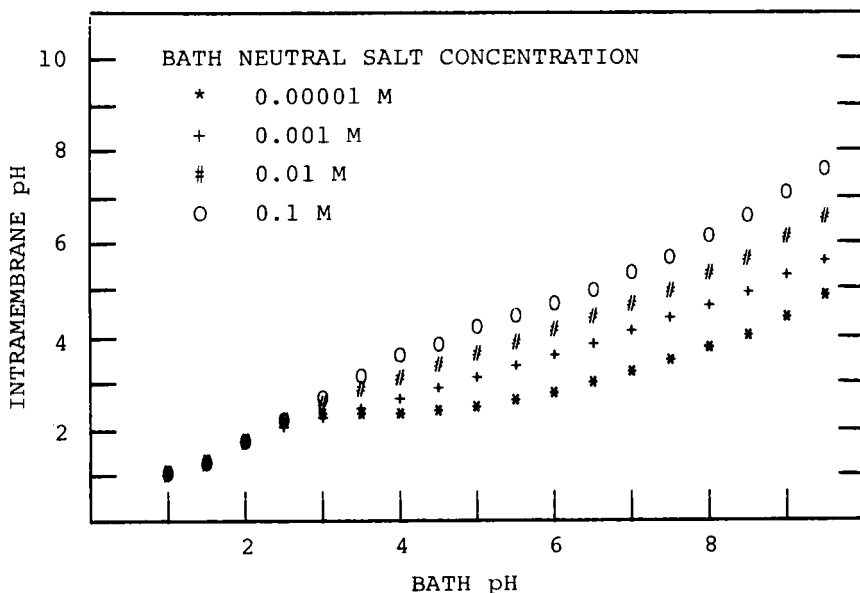


FIGURE 14

Effect of bath neutral salt concentration on the intramembrane pH, computed for a PMAA membrane (effective  $pK = 5.5$ ) based on Donnan theory (see Ref. 40 for method).

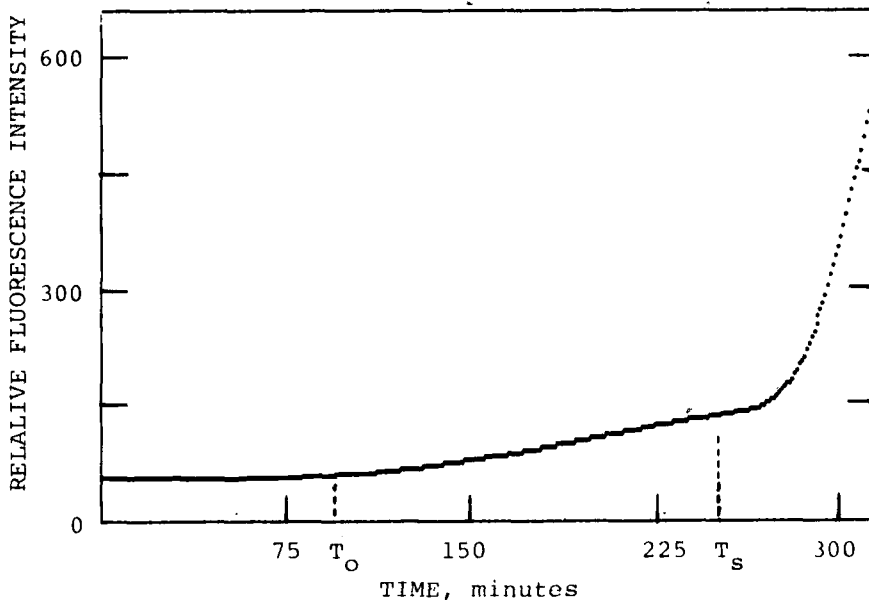


FIGURE 15

Effect of neutral salt concentration on the transport of  $\text{dI}-\text{C}_3\text{SO}_3^-$ -(5) across a PMAA membrane (0.25 ml glycerol per 50 ml 3.3% PMAA solution). After addition of KOH at time  $T_o$ , the pH changed slowly from an initial value of  $\sim 3.3$  to a value of  $\sim 6$ . At time  $T_s$ , KCl was added, raising the final salt concentration to 0.05 M.

to the baths by far exceeded the salt induced screening of the membrane fixed charge. In this experiment, no salt was added initially. Therefore, when the bath pH was raised (by addition of a small volume of 1 M KOH at time  $T_o$ ) there were not enough positive ions in the baths to exchange with the intramembrane hydrogen (which is required to charge the membrane) and still maintain the required Donnan ratio. Still, dye transport was seen to increase after addition of KOH. However, upon raising the concentration of KCl to 0.05 M at time  $T_s$ , the permeability increased dramatically. A plot of the calculated intramembrane pH versus bath pH with bath

salt concentration as a parameter is shown in Figure 15.

In order to eliminate the need to account for Donnan partitioning of a solute dye as the membrane becomes charged, experiments using neutral dyes have begun. Preliminary results with a net neutral zwitterion ( $I-C_3SO_3^- == I-C_1-(5)$ ) showed large, reversible changes in permeability which were consistent with the results obtained with charged dyes. However, adsorption of this neutral dye onto the chamber walls competed with transmembrane dye transport, making quantitative comparisons with other data more difficult.

#### VI. SUMMARY

This review has focused on membrane systems whose effective pore size can be changed in real time, thereby altering membrane permeability to neutral or charged solutes. Results show that membrane permeability to neutral solutes can be changed by application of an electric field across the membrane. Several techniques and mechanisms have been described, including an electrodiffusion mechanism in which the membrane supports a suitable ionic gradient. Recent measurements of pH-induced membrane permeability changes show that the magnitude of such permeability changes can be very large (orders of magnitude), and is reversible. Real-time fluorescence techniques, have been found to greatly facilitate the matching of membrane-solute pairs which maximize the change in permeability.

#### ACKNOWLEDGEMENTS

The authors would like to acknowledge the support of NSF Grant ENG 79-18781. Professor A. S. Waggoner, Carnegie Mellon University, provided samples of fluorescent dyes and Professor C. Warde provided laboratory facilities. J. N. Brenner of the Continuum Electromechanics Group performed the dextran transport experiments of Table I, and J. H. Nussbaum provided the PMAA membranes and the data of Figures 2 and 3. AMW is supported by a Fannie and John Hertz Foundation fellowship.

## REFERENCES

1. C.J. van Oss, *Separation and Purification Methods*, 8(2), 119 (1979).
2. S.R. Eisenberg and A.J. Grodzinsky, *J. Mem. Sci.*, 19, 173 (1984).
3. E. Pefferkorn, A. Schmitt, and R. Varoqui, *Biopolymers*, 21, 1451 (1982).
4. A. Bartollini, A. Gliozi, and I.W. Richardson, *J. Mem. Biol.*, 13, 283 (1973).
5. A. Gliozi, M.A. Penco, M. Battezzati, and A. Ciferri, *J. Mechanochem. Cell Motility*, 2, 219 (1973).
6. A. Gliozi, V. Vittoria, and A. Ciferri, *J. Mem. Biol.*, 8, 149 (1972).
7. D. Puett, A. Ciferri, and L. Rajagh, *Biopolymers*, 3, 439 (1965).
8. J.H. Bowes and R.H. Kenten, *Biochem. J.*, 43, 365 (1948).
9. N.A. Shoenfeld and A.J. Grodzinsky, *Biopolymers*, 19, 241 (1980).
10. A.J. Grodzinsky and S.R. Eisenberg, *J. Electrostatics*, 5, 33 (1978).
11. L.K. Shatayeva, G.V. Samsonov, J. Vacik, J. Kopecek, and J. Kalal, *J. App. Poly. Sci.*, 23, 2245 (1979).
12. J.H. Nussbaum, *Ph.D. Thesis*, MIT, 1985.
13. Y. Osada and Y. Saito, *Die Makromolekulare Chemie*, 176, 2761 (1975).
14. J. Vacik and J. Kopecek, *J. Appl. Poly. Sci.*, 19, 3029 (1975).
15. V. Kudela, J. Vacik, and J. Kopecek, *J. Mem. Sci.*, 6, 123 (1980).
16. Y. Osada and Y. Takeuchi, *J. Poly. Sci. Poly. Let. ed.*, 19, 303 (1981).
17. Y. Osada, *J. Poly. Sci. Poly. Chem. Ed.*, 15, 255 (1977).
18. Y. Osada and M. Sato, *Polymer*, 21, 1057 (1980).
19. R.S. Langer and N.A. Peppas, *Biomaterials*, 2, 201 (1981).

20. J. Kost, T.A. Horbett, B.D. Ratner and M. Singh, Glucose-sensitive membranes containing glucose oxidase: activity, swelling and permeability studies, *J. Biomed. Mater. Res.*, (in press).
21. T.A. Horbett, J. Kost, and B.D. Ratner, *ACS Polymer Preprints*, 24, 34 (1983).
22. K. Bala and P. Vasudevan, *J. Pharmaceutical Sci.*, 71, 960 (1982).
23. Trauble, H. and Eibl, H., in "Functional Linkage in Bimolecular Systems", F.O. Schmitt, D.M. Schneider, and D.M. Crothers, eds., Raven Press, New York, 1975, chap. 3.
24. Wieth, J.O., Brahm, J., and Funder, J., *Annals New York Acad. Sci.*, 341, 394 (1980).
25. A.L. Hodgkin, "The Conduction Of The Nervous Impulse", Charles C. Thomas, publisher, Springfield, Illinois, 1967.
26. in R.A. Nystrom, "Membrane Physiology", Prentice Hall, New Jersey, 1973, p. 52.
27. Goldman, D.E., in "Biophysics and Physiology of Excitable Membranes", W.J. Adelman, Jr. ed., Van Nostrand Reinhold, 1971, chap. 17.
28. M. Blank, in "Structure and Function in Excitable Cells", Chang, Tasaki, Adelman, and Leuchtag, eds., Plenum Pub. Corp., New York, 1983, 435.
29. N. Oyama and F.C. Anson, *J. Electroanal. Chem. Interfacial Electrochem.*, 127, 247 (1980).
30. I. Rubenstein and A.J. Bard, *J. Am. Chem. Soc.*, 103, 5007 (1981).
31. D.J. Harrison, K.A. Daube, and M.S. Wrighton, Behavior of metallic electrodes modified with a polymer derived from 4-( $\beta$ -trimethoxysilyl)ethylpyridine, *J. Electrochem. Soc.*, (in press).
32. A.N.K. Lau and L.L. Miller, *J. Am. Chem. Soc.*, 105, 5271 (1983).
33. P. Burgmayer and R.W. Murray, *J. Am. Chem. Soc.*, 104, 6139 (1982).
34. P. Burgmayer and R.W. Murray, *Proc. Electrochem. Soc. Meeting*, 83-1, 938 (1983).

35. V.A. Pasechnik, A.N. Cherkasov, V.P. Zhemkov, V.V. Chechina, and R.S. Alimardanov, *Kolloidnyi Zhurnal*, 41, 586 (1979).
36. J.D. Henry Jr., L.F. Lawler., and C.H.A. Kuo., *AIChE J.*, 23, 851 (1977).
37. J.M. Radovich and R.E. Sparks, in "Polymer Science and Technology" vol.13, A.R. Cooper, ed., Plenum Press, New York, 1980, 249.
38. R.A. Arndt and L.D. Roper, "Simple membrane electrodiffusion theory", *Physical Biological Sciences Misc.*, Blacksburg Va., 1972.
39. A.J. Grodzinsky and N.A. Shoenfeld, *Polymer*, 18, 435 (1977).
40. J.H. Nussbaum and A.J. Grodzinsky, *J. Membrane Sci.*, 8, 193 (1981).
41. S.R. Eisenberg and A.J. Grodzinsky, "Proc. 8th New England Bioengineering Conf.", I. Paul, ed., IEEE cat. no. 80 CH1574-3, Boston, MA, March, 1980, p. 240.
42. A.M. Weiss, Ph.D. Thesis, MIT, 1985.
43. K.S. Cole, *Physiol. Rev.*, 45, 340 (1965).
44. A.J. Grodzinsky, *CRC Crit. Rev. Biomed. Eng.*, 9, 133 (1983).
45. J.M. Valleton, Ph.D. Thesis, Facultes des Sciences de L'Universite de Rouen, 1984.
46. J.M. Valleton, J.C. Vincent, and E. Selegny, *Biophys. Chem.*, 15, 235 (1982).
47. E. Selegny, J.M. Valleton, and J.C. Vincent, *Bioelectrochem. Bioenergetics*, 10, 133 (1983).
48. J.L. Anderson and J.A. Quinn, *Biophys. J.*, 14, 130 (1974).
49. P.J. Sims, A.S. Waggoner, C.H. Wang, and J.F. Hoffman, *Biochemistry*, 13, 3315 (1974).
50. J. Crank, "The Mathematics of Diffusion", 2nd ed., Oxford University Press, Bristol, 1975, p. 51.
51. T. Teorell, *Prog. Biophys. Biophys. Chem.*, 3, chapter 9, (1953).
52. Y. Kobatake and N. Kamo, *Prog. Polymer Sci. Japan*, 5, 257 (1973).
53. F. Helfferich, "Ion Exchange", McGraw-Hill, New York, 1962.

54. T. Teorell, *J. Gen. Physiol.*, 42, 831 (1959).

55. A.J. Grodzinsky and J.R. Melcher, *IEEE Trans. Biomed. Eng.*, BME-23, 421 (1976).

#### APPENDIX

In general, ion concentration profiles within a membrane are determined by a balance between the competing processes of ion migration due to the presence of an electric field, diffusion due to a concentration gradient, and convection if there is fluid flow within the membrane. To solve for the intramembrane profiles, the continuity and flux laws, respectively, must be written for each of the  $i^{th}$  ionized species,

$$\frac{\partial \bar{c}_i}{\partial t} = - \frac{\partial \bar{r}_i}{\partial x} + (G_i - R_i) \quad (5)$$

$$\bar{r}_i = -D_i \frac{\partial \bar{c}_i}{\partial x} + \frac{z_i}{|z_i|} \bar{u}_i \bar{c}_i E_x + \bar{c}_i (v_x - v_m) \quad (6)$$

and combined with Gauss' law relating the electric field to the concentration of fixed and mobile charges:

$$\frac{\partial}{\partial x} (\epsilon E_x) = \bar{\rho} \quad (7)$$

$$\bar{\rho} = \bar{\rho}_m + F \sum_i z_i \bar{c}_i \quad (8)$$

where  $\bar{r}_i$ ,  $G_i$ , and  $R_i$  are the intramembrane flux, generation rate and recombination rate of the  $i^{th}$  species, respectively,  $\epsilon$  is the interstitial fluid dielectric constant,  $\bar{\rho}$  the total charge density (membrane charge  $\rho_m$  plus electrolyte), and  $v_x$  and  $v_m$  are the velocities of the fluid and membrane, respectively.

Equations (5) through (8) constitute a complete description

of the concentration and charge profiles assuming that the fluid velocity profile within the membrane is known. This system of equations is coupled and nonlinear, and has no closed form analytical solution. However, the experimental conditions of interest may justify several approximations which can lead to simplifying analytical solutions. Important issues here include the presence or absence of supporting electrolytes and, if the membrane itself contains fixed charge groups, the relative concentration of fixed and mobile charge species within the membrane. Theoretical modeling of such a problem has been investigated previously for the case of uniformly charged ion exchange and polymeric membranes<sup>51-53</sup> and for certain classes of biological membranes.<sup>54</sup>

For NaCl concentrations of interest at pH 2.8, the concentration of the membrane's positive fixed charge groups was much greater than the salt concentration in either half cell. Thus, Na<sup>+</sup> and H<sup>+</sup> were both coions (minority carriers); there was no other supporting electrolyte. Furthermore, since the membrane thickness was much greater than a Debye length  $1/\kappa = [\epsilon RT/(\Sigma z_i^2 F^2 c_{10})]^{1/2}$ , quasineutrality could be assumed to hold inside the membrane. These conditions decouple Gauss' law (7) from the coion continuity equations. Therefore, the intramembrane concentration profile can be found separately for each coion to a good approximation by incorporating the applied field  $E_0$  into its own continuity law (for example, equation (1)).

Grodzinsky and Shoenfeld<sup>39</sup> also considered other mechanisms by which an applied field could affect the membrane or ionic fluxes within it. The possibility that the field could cause a bulk electrokinetic translation of the non-rigid membrane was included by writing ion continuity relations in the frame of the membrane: that is, by using the convective derivative  $D/Dt = [\partial/\partial t + v_m(\partial/\partial x)]$ , where  $v_m$  is the membrane velocity. In addition, the applied electric field could induce fluid flow within the membrane by means of electroosmosis, as has been observed with porous glass frits<sup>54</sup> as well as collagen membranes.<sup>55</sup> Hence, an additional term for convective flux (with respect to the membrane) was added to each ion continuity relation (for example, equation (6)).